This article is part of the

Proceedings of the 16th Minisymposium Verfahrenstechnik and 7th Partikelforum (TU Wien, Sept. 21/22, 2020)

Title:
Diclofenac Removal and Fouling Behaviour of Multi-Channel Mixed Matrix Membranes (MCMMM) with Activated Carbon

Corresponding author:
Jan Back (MCI - The Entrepreneurial School), jan.back@mci.edu

Date of submission:
06.08.20

Date of revision:
25.08.20

Date of acceptance:
27.08.20

Chapter ID:
DiV1-(04)

Length:
7 pages

ISBN (full book):
978-3-903337-01-5

Diclofenac Removal and Fouling Behaviour of Multi-Channel Mixed Matrix Membranes (MCMMM) with Activated Carbon

J. Back[1,*], M. Spruck[1], M. Koch[1], S. Penner[2]

1: Department of Environmental, Process & Energy Engineering, MCI–The Entrepreneurial School, Maximilianstrasse 2, 6020 Innsbruck, Austria
2: Institute of Physical Chemistry, University of Innsbruck, Innrain 52c, 6020 Innsbruck, Austria
* Corresponding author: jan.back@mci.edu

Keywords: Micropollutant, Multi-channel membrane, Mixed matrix membrane, Activated carbon, Membrane fabrication, Fouling

Abstract

Anthropogenic micropollutants represent a major threat to the environment and more efficient removal processes are required. Drawbacks in the isolated application of either activated carbon or membrane technology resulted in this study where activated carbon is embedded into the matrix of a multi-channel membrane. The successful fabrication of such multi-channel mixed matrix membranes (MCMMM) from different main polymers (PES and PVDF) in a steam-dry-wet spinning process was complemented with diclofenac (DCF) removal rates of up to 65 % after 60 min. The compatibility of the filler material with the membrane matrix was variable: The PES support structure seemed to disintegrate with the addition of >2 % AC, whereas PVDF showed better interaction with the filler and burst pressures of >3.5 bar. Humic acid filtration with PVDF-based MCMMM and 3 % AC added to the spinning solution showed a reduction of the normalized flux by 24 % – a slight improvement compared to 29 % reduction in the case of the pristine PVDF membrane. The fouling behaviour could be described with a semi-empirical model. Altogether, MCMMM are a promising approach for the efficient removal of micropollutants.

Introduction

Nowadays, dissolved organic micropollutants can be found in nearly all European streams [1]. Examples of these micropollutants are pharmaceuticals, hormones, pesticides and industrial chemicals, which – despite their low concentration being in the micro- to nanogram per litre-range – are detrimental to aquatic ecosystems [2]. If drinking water is produced from these waters, damage to humans cannot be ruled out [3]. Wastewater treatment plants (WWTP) do not fully degrade harmful micropollutants, even if the state-of-the-art activated sludge technology is applied [4]. Hence, research efforts are directed towards removing these micropollutants using different technologies, of which the most important ones are activated carbon adsorption and ozonation [5,6]. Switzerland's legislation has responded to the rising micropollutant load in the environment by upgrading over 100 WWTP in an investment of 1.2 billion CHF, whereas in the EU, lawmakers have been more conservative; so far, mostly regional efforts (e.g. in Baden-Württemberg or Nordrhein-Westfalen, Germany) have been initiated [7].

In the past decades, membrane technology has developed into one of the most important technologies to remove colloids and dissolved substances from water [8]. According to the principle of size exclusion, the feed solution is separated into permeate and retentate. However, for an effective removal of these micropollutants through membrane technology, very small pore sizes and, consequently, high energy cost would be required.

Mixed matrix membranes (MMM) are a relatively new research field, in which filler materials are combined with – usually polymeric – membranes matrices for either liquid or gas separation [9,10]. A variety of organic and inorganic fillers have been used, and activated carbon (AC) MMM – due to their enhanced characteristics – are a strong contender to conventional membranes [11]. Besides potential enhancement of the membrane surface properties such as hydrophilicity, porosity, and surface roughness by utilizing AC for MMM synthesis, the excellent adsorption capacity of AC allows for the combination of an adsorptive stage and a filtration step in one single process [11].

A wide range of applications of AC MMM has been reported in the literature. The removal of ionic components such as heavy metals [12–16] and uranium [17,18] has been described. In terms of aromatic organic compounds, AC MMM have been used for phenol removal [19,20] as well as benzene and toluene elimination [21]. Further research has been conducted on dairy wastewater treatment [22], *E. coli* removal [23], and blood toxin removal [24,25]. In addition, the removal of organic micropollutants has been mentioned in several studies on flat sheet membranes with diverse realisations to combine the two processes (e.g. dual layer membranes) have been described [26–31].

Regarding the MMM fabrication process, the filler materials are normally dispersed in the casting solution and then processed in a phase inversion process, where either flat sheet or hollow fibre membranes are obtained. The phase inversion may be induced by evaporation (dry phase inversion), by immersion precipitation (wet phase inversion), or a combination of the two. Other techniques create two-layer membranes by using co-casting knives or dual layer spinnerets.

Multi-channel membranes provide an appealing geometry, as their mechanical stability is enhanced and the filtration area to volume ratio may be superior compared to their single-channel counterparts [32]. Moreover, the high shear forces at the channel surfaces may induce a fouling mitigation [33], tackling one of the biggest drawbacks in the application of membrane technology.

The aim of this research was the fabrication of multi-channel mixed matrix membranes (MCMMM) for the removal of micropollutants from different spinning solution compositions using the common painkiller diclofenac (DCF) as model micropollutant. The influence of AC addition on the mechanical stability of the MCMMM was also investigated. Moreover, the potential enhancement of the membrane surface properties in terms of fouling reduction was evaluated by fouling experiments using humic acid, and by applying a semi-empirical modification of the resistance-in-series model.

Materials and Methods

Membrane fabrication

In the first step of the membrane fabrication process, polymeric solutions were prepared by homogenizing the main polymer (polyethersulfone (PES, Ultrason E 3020 P, BASF) or polyvinylidene fluoride (PVDF, Solef 1015, Solvay)), the additives (polyvinylpyrrolidone (PVP) with different M_w (10 or 360 kDa) and/or propane-1,2-diol (PD)), and the solvent (*N,N*-

dimethylacetamide (DMAc)). These polymeric solutions are the result of previous optimizations [32,34]. Pre-dried activated carbon (AC, Carbopal AP supra, Donau Carbon) as solid filler material and adsorbent (d_{10} = 4.7 µm, d_{50} = 26.1 µm, d_{90} = 74.8 µm [35]) was then added to the solution. This solution was stirred carefully at 30 rpm for 30 min and sonicated for 15 min, in order to achieve an outgassed and homogeneous polymer-AC-solution (Tab. 1). The reference quantity was the polymeric solution (e.g. 300 g), to which AC was added in the reported percentages (e.g. + 3 g for + 1 % AC). It is assumed that the main polymer (PES or PVDF) and the co-polymer (PVP) form the solid membrane matrix and that the AC is embedded into that matrix; the AC content with respect to the total solids hence varied between 4.0 and 25.9 %. As the additive content was not varied, the membrane batches are referred to by their main polymer content and their AC content (e.g. 15 % PES/1 % AC) hereinafter. The rheology of the polymer-AC-solutions was analysed with a rotational viscometer at shear rates between 10 and 500 s^{-1} and 20 °C.

The multi-channel membranes were prepared in a steam-dry-wet spinning process with an advanced, 7-bore spinning nozzle (Fig. 1 a,b) via non-solvent induced phase inversion. The polymer-AC solutions were processed in the spinning process directly after production to prevent particle settling. Water at 30 °C was applied as bore fluid, i.e. internal coagulant. The external coagulant was also H_2O at 30 °C. Further details concerning the fabrication process are described elsewhere [32,34].

Membrane characterization

The membrane pure water flux J and permeability P were determined at 25 °C and 1 bar transmembrane pressure (TMP) with a membrane testing plant applying an inside-out crossflow operation mode (Fig. 1c) with single-fibre modules.

For macromolecule retention R measurements, 1 g L^{-1} dextrane (500 kDa) solutions were filtered at 25 °C and 1 bar TMP. The concentrations in the feed and in the permeate were determined with a TOC analyser.

Micropollutant retention R was tested via filtration of 15 mg L^{-1} DCF sodium salt-solutions (25 °C, 1 bar, feed flow rate: 40 L min^{-1}). The feed and permeate concentrations were measured with an acetonitrile/5 mmol L^{-1} phosphoric acid gradient HPLC with a reverse phase column at 278 nm, as described in [35].

The mechanical strength of the MCMMM was evaluated in terms of burst pressure and tensile strength.

The morphology was investigated using scanning electron microscopy (SEM) at 20x and 150x magnification, respectively, and at an acceleration voltage of 15 kV.

Fouling behavior

The MCMMM fouling susceptibility of PVDF MCMMM was studied by filtering a humic acid solution. The resistance-in-series model – derived from Darcy's law – was applied for the semi-empirical time-dependent analysis of the fouling behavior (Eq. 1) [36]:

$$J_t(t) = \frac{\Delta p}{\eta\, R_t(t)} = \frac{\Delta p}{\eta\,(R_m + R_{if} + \underbrace{R_{cp}(t) + R_c(t)}_{R_f})} \quad (1)$$

Here, η is the dynamic viscosity, R_t is the total resistance, and R_m is the hydraulic resistance of the clean membrane – a constant value regardless of the operation conditions. R_{if} is the resistance of internal fouling resulting from the adsorption

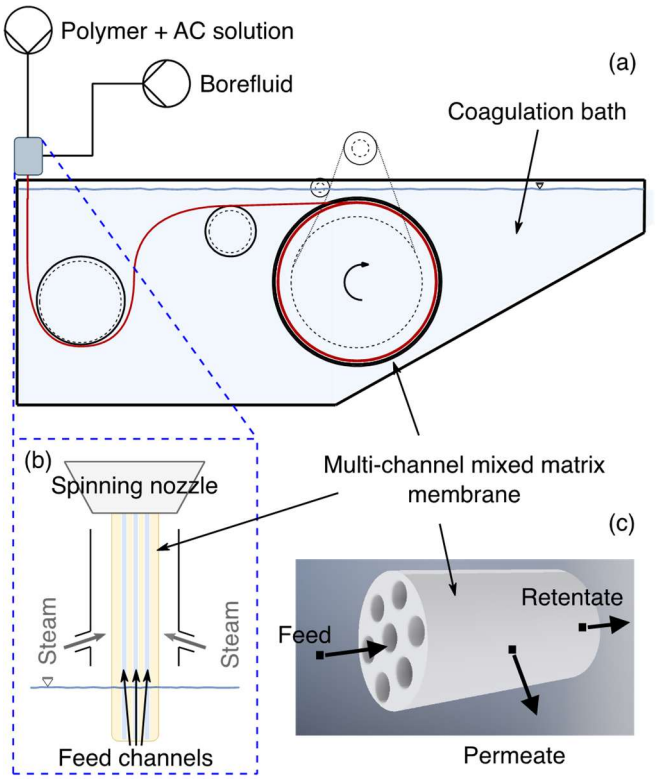

Fig. 1: MMMCM production process via non-solvent induced phase inversion (a), spinning nozzle (b) and MCMMM operation mode (c).

Tab. 1: Compositions of polymer-AC-solution for steam-dry-wetting spinning.

Main polymer, content	Additives, content	Solvent, content	AC content
PES 13 %	PVP 360 kDa 5 %, PD 15 %	DMAc 67 %	+ 3 %
PES 15 %		DMAc 65 %	
PES 17 %		DMAc 63 %	
PES 19 %		DMAc 61 %	
PES 21 %		DMAc 59 %	
PES 15 %	PVP 360 kDa 5 %, PD 15 %	DMAc 65 %	+ 0 %
			+ 1 %
			+ 2 %
			+ 3 %
			+ 4 %
			+ 5 %
			+ 7 %
PVDF 18 %	PVP 10 kDa 6 %	DMAc 76 %	+ 0 %
			+ 1 %
			+ 2 %
			+ 3 %
			+ 4 %
			+ 5 %

of fine fouling material on the inside of the membrane pores – assumed to occur instantaneously at the beginning of the filtration and not to be significantly influenced by the operating conditions [37,38]. R_{cp} is the resistance resulting from concentration polarization, and R_c is the resistance from the formed cake layer on the membrane surface. R_{cp} and R_c are the main components for the fouling resistance during operation; however, as the calculation of separate values is challenging, they are combined into R_f.

In order to determine said resistances, firstly, the pure water flux J_{pw} was measured (25 °C, 1 bar) and the hydraulic membrane resistance R_m is calculated (Eq. 2) [36].

$$J_{pw} = \frac{\Delta p}{\eta\, R_m} \quad (2)$$

Secondly, the humic acid solution (1 g L^{-1}, 25 °C) was used as feed solution and the flux J_0 was recorded after stably adjusting the operation conditions to 40 L min^{-1} feed flow rate and 1 bar TMP for typically 5 min. The declining flux J was determined in intervals for a filtration period of 240 min at a constant TMP of 1 bar. The internal fouling resistance R_{if} is calculated, assuming that fine fouling material is adsorbed instantaneously (Eq. 3).

$$J_t(t=0) = J_0 = \frac{\Delta p}{\eta\, R_{t_0}} = \frac{\Delta p}{\eta\,(R_m + R_{if})} \tag{3}$$

The subsequent and more complex step is the estimation of the time-dependent part of the fouling resistance R_f. It is assumed that in a cross-flow process, the resistance will approach a steady-state behavior after time (Eq. 4).

$$\lim_{t\to\infty} R_f(t) = R_{fss} \tag{4}$$

The change of the fouling resistance with time is described via a pseudo first-order rate law (Eq. 5 and 6) [39,40].

$$\frac{\mathrm{d}R_f(t)}{\mathrm{d}t} = -k\,(R_{fss} - R_f(t)) \tag{5}$$

$$R_f(t) = R_{fss}\,(1 - \exp(-k\,t)) \tag{6}$$

Inserting Eq. 4 and 6 into Eq. 1 yields Eq. 7 – the time-dependent description of the flux, and Eq. 8 – the normalized flux.

$$\lim_{t\to\infty} J_t(t) = J_{tss} = \frac{\Delta p}{\eta\, R_{tss}} = \frac{\Delta p}{\eta\,(R_m + R_{if} + R_{fss})} \tag{7}$$

$$\frac{J_t(t)}{J_0} = \frac{1}{1 + \underbrace{\frac{R_{fss}}{R_m + R_{if}}}_{b}\,(1 - \exp(-k\,t))} \tag{8}$$

The latter equation is applied for parameter fitting of b and k to the normalized flux over time using R [41]. The estimation of b subsequently allows for the calculation of the steady-state fouling resistance R_{fss}.

Results and Discussion

Membrane characteristics

MCMMM were successfully fabricated in a steam-dry-wet spinning process from polymeric solutions with suspended AC particles via non-solvent induced phase inversion. SEM images (Fig. 2) reveal a clean and uniform formation of the seven feed bores and the outer wall, and the diameters are in the range of the spinneret dimensions. AC was uniformly distributed and seemingly well embedded in the membrane matrix (Fig. 2 c-d, g-h), and AC particles, in the expected dimensions (d_{10} = 4.7 µm, d_{50} = 26.1 µm, d_{90} = 74.8 µm), were clearly visible in the SEM images (Fig. 2 c-d, g-h), which may point to particle integrity, or the absence of particle breakage during the production process, as opposed to previous studies [42]. The tendency of AC particles to settle near the membrane wall has been described before [20–22], but could not be confirmed for MCMMM. This could imply a favourable polymer-filler interaction and signify enhanced adsorption characteristics of micropollutants. However, the SEM images do not clearly indicate whether the pore structure of the AC is affected by the main polymers, the additives, or the solvent. This would impair the adsorption capacity of the AC and, hence, deserves further attention.

For the case of PES being the main polymer (Fig. 2 a-d), the addition of AC led to the formation of more macro-voids and a less uniform secondary structure. When PVDF was used as the main polymer (Fig. 2 e-h), the finger-like structure of the pristine membrane remained largely unchanged by the addition of AC, both at the active filtration layer and in the secondary structure. This may indicate a better compatibility of the filler material and the PVDF-based membrane matrix.

The filtration performance was evaluated in terms of pure water permeability P and macromolecule retention R (Fig. 3 a-c). The membrane permeability ranged from 18 to 175 LMH bar^{-1}, and the dextrane 500 kDa retention varied between 43 and 84 %, indicating that the membranes be classified at the borderline between micro- and ultrafiltration. While a clear trend is apparent for a main polymer content variation (Fig. 3a) – a higher content leads to denser and less permeable structures [8] – the addition of AC does not imply an obvious tendency. This may suggest that the active filtration layer – which is mainly responsible for the filtration performance – is not altered substantially through the addition of AC within the reported range.

The permeability/retention-trade-off is mostly, but not always represented. The formation processes of both mixed matrix and multi-channel membranes, and particularly the combination of the two, are highly complex. This deviation from the commonly accepted P/R-trade-off in some cases may indicate that unknown variables, which were not adequately controlled during the presented membrane manufacturing and characterization process, have a potential influence on the shown data. These potential “white spots on the MCMMM-map” should be eliminated in an extensive parameter study in order to further the understanding of this complex process.

Regarding DCF retention over time (Fig. 3 d-f), the effectiveness of MCMMM for micropollutant elimination is clearly shown in the comparison with pristine membranes. As small micropollutant molecules such as DCF are not retained by ultrafiltration membranes, the adsorbent availability of the embedded activated carbon is demonstrated. However, it remains unclear whether the adsorption capacity is altered due to changes in the pore structure of the adsorbent during the mixed matrix membrane production process.

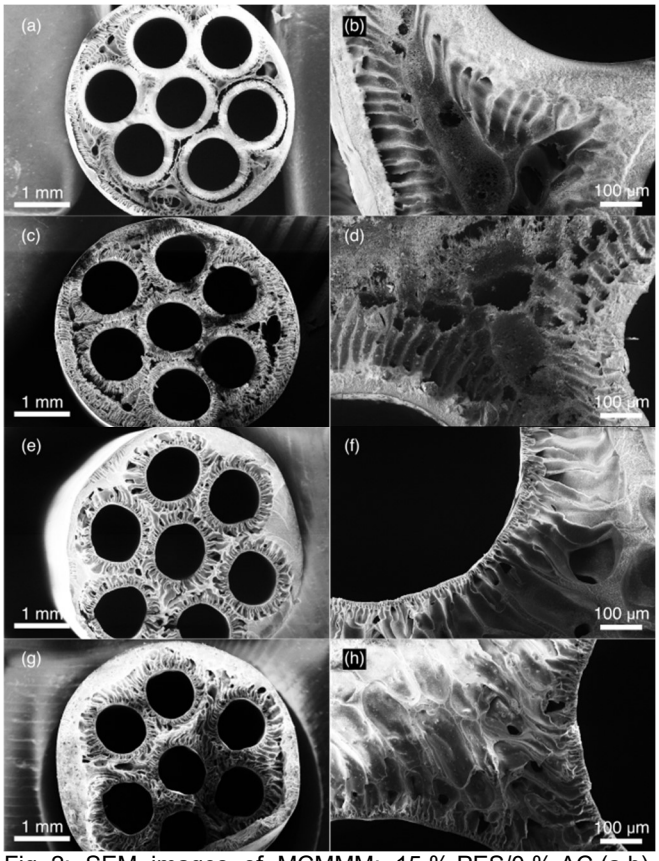

Fig. 2: SEM images of MCMMM: 15 % PES/0 % AC (a,b), 15 % PES/5 % AC (c,d), 18 % PVDF/0 % AC (e,f), 18 % PVDF/5 % AC (g,h).

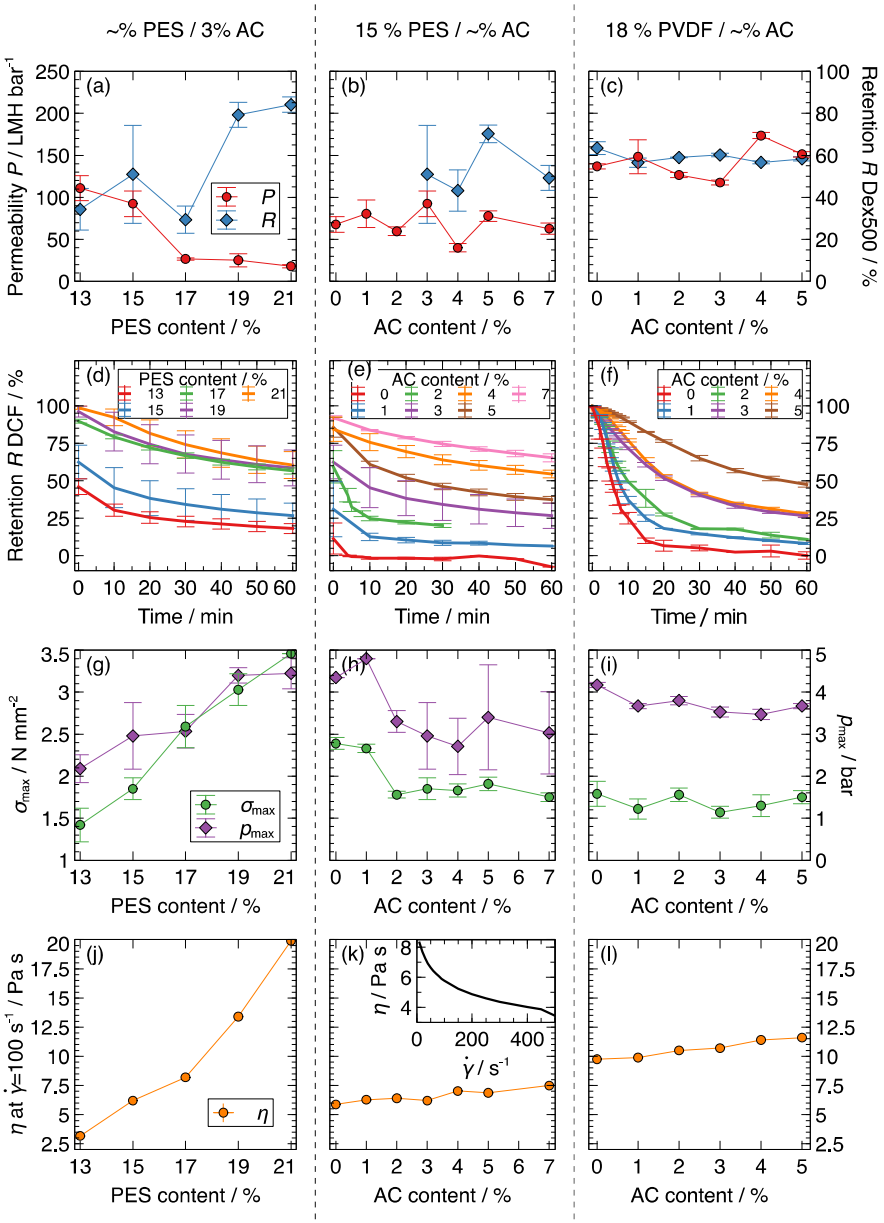

Fig. 3: Filtration performance (a-c), micropollutant removal (d-f), and mechanical stability (g-i) of MCMMM; rheological analysis of corresponding polymer solutions (j-l) with typical shear-rate dependency (inset in (k) – 15 % PES/7 % AC).

Retention values decrease over time, which is ascribed to firstly, approaching the adsorption capacity of each membrane and, secondly, to smaller gradients in the adsorption process, which results in slower kinetics. For mixed matrix membranes, the DCF retention after 60 min decreases to 7–65 %, which indicates that the maximum adsorption capacity of the adsorbent is not reached in the studied timeframe. In typical feeds such as WWTP effluents or even industrial effluents, the micropollutant concentration is much lower than in the presented study – for WWTP effluent a mean DCF concentration of 260–647 ng L^{-1} was found [43]. The potabilization of surface water – another envisaged application – faces even lower DCF concentrations; an average of 17 ng L^{-1} was found for European rivers. A better retention for such diluted feed solutions is expected, even though a great variety of pollutants and other substances may be present; a field study is suggested to investigate the elimination of a wider range of micropollutants from more complex solutions.

It is noted that a higher PES content – i.e. a denser membrane – led to a higher DCF retention (Fig. 3d). The reason for this observation must be sought in transport mechanisms: A denser membrane exhibits a lower permeability (Fig. 3a) as well as – at constant pressure – a higher dwell time of the feed solution in the membrane matrix. The dimensions of the diffusion layers of the adsorption process are expected to remain largely unchanged, as the flow in the membrane matrix is laminar in any case [8]. Hence, a higher dwell time will increase the likelihood of a DCF molecule to diffuse into the AC particle and to be adsorbed.

Furthermore, an increase in adsorbent content generally resulted in a higher DCF retention (Fig. 3 e-f). The pristine membranes showed a decline to under 5 % retention in the first 10 or 40 min for PES and PVDF, respectively. This seemingly higher adsorption capacity for pristine PVDF membranes may be due to the fact that PVDF is the more hydrophobic polymer, due to the lower molecular weight of the co-polymer PVP in the fabricated PVDF membranes, or a combination of both.

Exceptions to the general trend are the membranes 15 % PES/4 % AC and 15 % PES/5 % AC – the batch with the higher AC content has a lower retention over time. The permeability of these two batches in Fig. 3b follows an opposing trend: The batch with the higher AC content exhibits a higher permeability, which corroborates the si-gnificance of

membrane density – a denser membrane batch may lead to higher dwell times and enhanced micropollutant elimination behaviour, even though the total adsorption capacity is lower. Micropollutant elimination by MCMMM thus represents a complex interplay of membrane density, dwell time, adsorbent content, adsorbent availability, adsorption capacity, adsorption kinetics, and potentially further factors. The presented study may hence be considered as a proof of principle, but the elucidation of the micropollutant removal mechanisms requires further research.

In terms of mechanical stability (Fig. 3 g-i), most membranes withstand the typical pressure applied in micro-/ultrafiltration of 2 bar. Again, a higher main polymer content leads to denser and, in this case, more sturdy membranes. The AC addition of 2 % or more to the membrane matrix leads to a significantly diminished mechanical stability for PES. This effect is less significant in the case of PDVF. It is also noted that PVDF membranes invariably show a burst pressure over 3.5 bar as opposed to PES membranes. The tensile strength of PVDF membranes, however, is invariably below 2 N mm^{-2}. This behaviour may be explained through differences in polymer-filler interactions: The properties of the hydrophobic polymer PVDF may be better compatible with the relatively hydrophobic AC compared to the polymer PES. The polymer-filler interaction is therefore enhanced in the case of PVDF MCMMM. This is in line with previously discussed SEM images (Fig. 2), in which a disintegrated secondary structure was observed for PES/AC MCMMM. This lack of connectivity in the support structure may be the root cause for diminished mechanical stability at filler contents > 2 %, whereas 1 % may be the limit for this polymer-filler system to remain stable. The generally lower tensile strength of PVDF membranes may be related to shorter main polymer and co-polymer chains. However, it should be mentioned that burst pressure is the prime mechanical characteristic when considering the application as a membrane filter, as tensile forces will rarely occur. Hence, PVDF may represent the more convenient choice of polymer in this case.

Rheological analysis of the polymer-AC-solutions (Fig. 3 j-l) revealed shear-thinning behaviour for all solutions (example shown in inset in Fig. 3k). The increase of PES expectedly increased the viscosity (Fig. 3j). The addition of AC only had a minor impact on the solution viscosity (Fig. 3 k-l), which may signify that from a rheological standpoint, the membrane production process follows similar rules when fillers are added. In other words, the maximum allowable viscosity for the spinneret and polymer pumps is mainly determined by the polymeric solution, not by the filler content. This maximum viscosity was approached for the case of 21 % PES/3 % AC, as higher PES contents resulted in an unstable manufacturing process. Furthermore, it is noted that the viscosity of the polymer solutions with 18 % PVDF (Fig. 3l) is similar to solutions with a comparable PES content (Fig. 3j). Nonetheless, the properties of the membranes vary significantly (e.g. permeability/retention, tensile strength). Hence, the membrane properties are not dominated by the viscosity alone and the choice of polymer must be tailored to the eventual filtration process requirements.

Fouling behaviour

As PVDF MCMMM display enhanced performance in terms of the permeability/retention-trade-off and regarding the burst pressure, they represent a promising prospect for the application as micropollutant elimination technology. In real feed solutions, however, varying quantities of fouling components may be present. The fouling behaviour of PVDF MCMMM was hence studied with humic acid (Fig. 4). The normalized permeate flux decreased over time to under 60 % of the original flux after 240 min for 1 and 5 % AC. MCMMM with 0, 2, 3, and 4 % AC performed slightly better; the flux declined to 65 to 80 %.

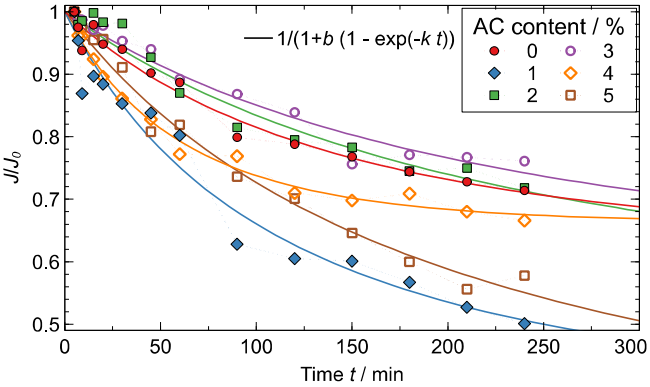

Fig. 4: Time dependency of normalized flux J/J_0 for 18 % PVDF/~AC MCMMM in humic acid (1 g L^{-1}, 1 bar) filtration.

A semi-empirical approach was chosen using a first-order rate law combined with the resistance-in-series model in order to describe the fouling behaviour and to investigate the different resistances. The models are plotted in Fig. 4 and the fitting parameters are tabulated in Tab. 2. The coefficient of determination r^2 is invariably >0.95, indicating that the behaviour may be adequately described by the selected approach. Although only a levelling-off of the flux, instead of a steady state flux, was observed within the studied time frame of 240 min, the flux – according to the chosen model –is expected to reach a constant value due to an equilibrium state of shear forces with the cross-flow and particle deposition. This behaviour is represented in the model parameter b, whereas k is the rate constant related to the time which is required to reach this steady state. The equilibrium steady-state flux is inversely proportional to the total resistance at the steady state predicted by the model R_{tss} (Fig. 5). The membrane resistance R_m is inversely proportional to the pure water permeability P in Fig. 3c.

The steady-state fouling resistance R_{fss} first increases after AC addition of 1 %, then decreases to the lowest value at 4 %, and finally escalates again at 5 % AC. On the other hand, the internal fouling R_{if} increases up to 4 % AC addition and decreases thereafter. A correlation between the fouling resistances in Fig. 5 and the membrane characteristics in Fig. 3 has not been observed. Fouling is a very complex phenomenon, which has been linked to many different influencing parameters, such as cross-flow velocity, hydrophobicity of the membrane surface, and surface roughness. Hydrophilization has been observed through the incorporation of AC in the membrane matrix [16]. Nonetheless, more research is suggested to understand the observed fouling behaviour. The best compromise between adsorption capacity and membrane fouling seems to be re-presented by the PVDF MCMMM with 3 and 4 % AC added.

Tab. 2: Fitting parameters for fouling of 18 % PVDF/~AC MCMMM during humic acid filtration.

AC content / %	k / min^{-1}	b / -	r^2
0	0.0048	0.592	0.976
1	0.0038	1.640	0.959
2	0.0026	0.862	0.963
3	0.0030	0.674	0.969
4	0.0120	0.509	0.986
5	0.0015	2.692	0.956

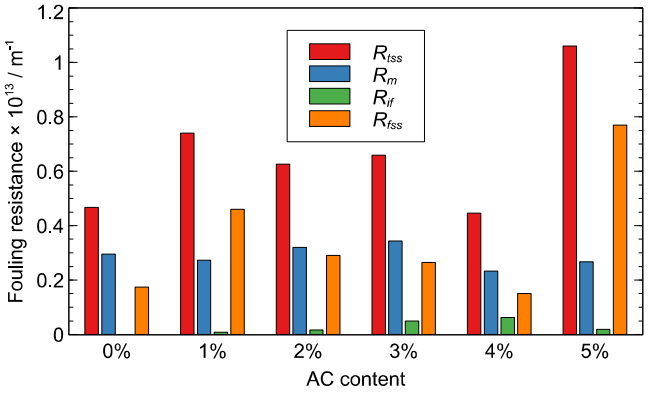

Fig. 5: Membrane fouling resistances for 18 % PVDF/~AC MCMMM determined from pure water filtration and modelled humic acid experiments.

Conclusion

In order to combat the challenge of rising micropollutant concentrations in the environment, MCMMM with embedded AC have been developed. Both of the tested main polymers PES and PVDF resulted in acceptable membrane structures, whilst PVDF seemed to be slightly better compatible with the added AC. The model pollutant DCF showed declining removal rates over time, with a maximum of 65 % removal after 60 min. The fouling behaviour with humic acid could be described with a semi-empirical model. The presented study should be considered a proof of principle for the application of MCMMM as micropollutant elimination technology, but further efforts should be directed to the elucidation of the fabrication process and the removal mechanisms as well as to the implementation of field and pilot studies.

Acknowledgements

This work was supported by the Government of Tyrol (Austria) via Tiroler Wissenschaftsfonds [grant number GZ: F. 16943/5-2019]. Assistance in laboratory experiments, methods description, and proofing provided by J. Eff, M. Hofer, S. Kostner, J. Steinberger, J. Tschugmell (MCI), and S. Agath (University of Innsbruck) is greatly appreciated.

References

[1] Loos, R., Gawlik, B. M., Locoro, G., Rimaviciute, E., Contini, S., and Bidoglio, G., “EU-wide survey of polar organic persistent pollutants in European river waters,” *Environ. Pollut.*, vol. 157, no. 2, pp. 561–568, 2009, doi: 10.1016/j.envpol.2008.09.020.

[2] Schwarzenbach, R. P. *et al.,* “The challenge of micropollutants in aquatic systems,” *Science*, vol. 313, no. 5790, pp. 1072–1077, 2006, doi: 10.1126/science.1127291.

[3] Pomati, F. *et al.,* “Effects of a Complex Mixture of Therapeutic Drugs at Environmental Levels on Human Embryonic Cells,” *Environ. Sci. Technol.*, vol. 40, no. 7, pp. 2442–2447, 2006, doi: 10.1021/es051715a.

[4] Clara, M., Strenn, B., Gans, O., Martinez, E., Kreuzinger, N., and Kroiss, H., “Removal of selected pharmaceuticals, fragrances and endocrine disrupting compounds in a membrane bioreactor and conventional wastewater treatment plants,” *Water Res.*, vol. 39, no. 19, pp. 4797–4807, 2005, doi: 10.1016/j.watres.2005.09.015.

[5] Bui, X. T., Vo, T. P. T., Ngo, H. H., Guo, W. S., and Nguyen, T. T., “Multicriteria assessment of advanced treatment technologies for micropollutants removal at large-scale applications,” *Sci. Total Environ.*, 563-564, pp. 1050–1067, 2016, doi: 10.1016/j.scitotenv.2016.04.191.

[6] Abegglen, C. and Siegrist, H., “Mikroverunreinigungen aus kommunalem Abwasser: Verfahren zur weitergehenden Elimination auf Kläranlagen,” Schweizerisches Bundesamt für Umwelt, Bern, Umwelt-Wissen 1214, 2012.

[7] KomS BW, KOM-M. NRW, VSA Plattform, *Tagungsband 5 Jahre Kompetenzzentren Spurenstoffe*. Friedrichshafen: DWA-BW, Jul. 2017.

[8] Strathmann, H., *Introduction to membrane science and technology*. Weinheim, Germany: Wiley-VCH Verlag & Co., 2011.

[9] Esfahani, M. R. *et al.,* “Nanocomposite membranes for water separation and purification: Fabrication, modification, and applications,” *Sep. Purif. Technol.*, vol. 213, pp. 465–499, 2019, doi: 10.1016/j.seppur.2018.12.050.

[10] Ebadi Amooghin, A., Mashhadikhan, S., Sanaeepur, H., Moghadassi, A., Matsuura, T., and Ramakrishna, S., “Substantial breakthroughs on function-led design of advanced materials used in mixed matrix membranes (MMMs): A new horizon for efficient CO2 separation,” *Prog. Mater. Sci.*, vol. 102, pp. 222–295, 2019, doi: 10.1016/j.pmatsci.2018.11.002.

[11] Lewis, J., Al-sayaghi, M. A. Q., Buelke, C., and Alshami, A., “Activated carbon in mixed-matrix membranes,” *Sep. Purif. Rev.*, pp. 1–31, 2019, doi: 10.1080/15422119.2019.1609986.

[12] He, J., Matsuura, T., and Chen, J. P., “A novel Zr-based nanoparticle-embedded PSF blend hollow fiber membrane for treatment of arsenate contaminated water: Material development, adsorption and filtration studies, and characterization,” *J. Membr. Sci.*, vol. 452, pp. 433–445, 2014, doi: 10.1016/j.memsci.2013.10.041.

[13] He, J., Song, Y., and Chen, J. P., “Development of a novel biochar/PSF mixed matrix membrane and study of key parameters in treatment of copper and lead contaminated water,” *Chemosphere*, vol. 186, pp. 1033–1045, 2017, doi: 10.1016/j.chemosphere.2017.07.028.

[14] Mohamad Said, K. A., George, G. G., Mohamed Alipah, N. A., Ismail, N. Z., and Jama’in, R. L., “Effect of Activated Carbon in Polysufone-Polyethyleneimine-Silver Composite Membrane Towards Adsorption of Chromium (Cr), Lead (Pb), Silver (Ag) and Cadmium (Cd) in Synthetic Wastewater,” *J. Mater. Environ. Sci.*, vol. 8, no. 11, pp. 3740–3746, 2017.

[15] Hofman, M. and Pietrzak, R., “Copper ions removal from liquid phase by polyethersulfone (PES) membranes functionalized by introduction of carbonaceous materials,” *Chem. Eng. J.*, 215-216, pp. 216–221, 2013, doi: 10.1016/j.cej.2012.10.079.

[16] Hosseini, S. M., Amini, S. H., Khodabakhshi, A. R., Bagheripour, E., and van der Bruggen, B., “Activated carbon nanoparticles entrapped mixed matrix polyethersulfone based nanofiltration membrane for sulfate and copper removal from water,” *J. Taiwan Inst. Chem. Eng.*, vol. 82, pp. 169–178, 2018, doi: 10.1016/j.jtice.2017.11.017.

[17] Villalobos-Rodríguez, R., Montero-Cabrera, M. E., Esparza-Ponce, H. E., Herrera-Peraza, E. F., and Ballinas-Casarrubias, M. L., “Uranium removal from water using cellulose triacetate membranes added with activated carbon,” *Appl. Radiat. Isot.*, vol. 70, no. 5, pp. 872–881, 2012, doi: 10.1016/j.apradiso.2012.01.017.

[18] Villalobos-Rodríguez, R. *et al.,* “Iron influence on uranium removal from water using cellulose acetate

membranes doped with activated carbon," *Desalin. Water Treat.*, vol. 56, no. 13, pp. 3476–3485, 2015, doi: 10.1080/19443994.2014.980333.

[19] Saranya, R., Kumar, M., Tamilarasan, R., Ismail, A. F., and Arthanareeswaran, G., "Functionalised activated carbon modified polyphenylsulfone composite membranes for adsorption enhanced phenol filtration," *J. Chem. Technol. Biotechnol.*, vol. 91, no. 3, pp. 748–761, 2016, doi: 10.1002/jctb.4641.

[20] Mukherjee, R. and De, S., "Preparation, characterization and application of powdered activated carbon-cellulose acetate phthalate mixed matrix membrane for treatment of steel plant effluent," *Polym. Adv. Technol.*, vol. 27, no. 4, pp. 444–459, 2016, doi: 10.1002/pat.3690.

[21] Mukherjee, R. and De, S., "Novel carbon-nanoparticle polysulfone hollow fiber mixed matrix ultrafiltration membrane: Adsorptive removal of benzene, phenol and toluene from aqueous solution," *Sep. Purif. Technol.*, vol. 157, pp. 229–240, 2016, doi: 10.1016/j.seppur.2015.11.015.

[22] Aghili, F., Ghoreyshi, A. A., Rahimpour, A., and Rahimnejad, M., "Coating of mixed-matrix membranes with powdered activated carbon for fouling control and treatment of dairy effluent," *Process Saf. Environ. Prot.*, vol. 107, pp. 528–539, 2017, doi: 10.1016/j.psep.2017.03.013.

[23] Hassan, M., Abou-Zeid, R., Hassan, E., Berglund, L., Aitomäki, Y., and Oksman, K., "Membranes Based on Cellulose Nanofibers and Activated Carbon for Removal of Escherichia coli Bacteria from Water," *Polymers*, vol. 9, no. 8, 2017, doi: 10.3390/polym9080335.

[24] Tijink, M. S. L. *et al.,* "A novel approach for blood purification: mixed-matrix membranes combining diffusion and adsorption in one step," *Acta. Biomater.*, vol. 8, no. 6, pp. 2279–2287, 2012, doi: 10.1016/j.actbio.2012.03.008.

[25] Tijink, M. S. L. *et al.,* "Mixed matrix hollow fiber membranes for removal of protein-bound toxins from human plasma," *Biomaterials*, vol. 34, no. 32, pp. 7819–7828, 2013, doi: 10.1016/j.biomaterials.2013.07.008.

[26] Nadour, M., Boukraa, F., and Benaboura, A., "Removal of Diclofenac, Paracetamol and Metronidazole using a carbon-polymeric membrane," *J. Environ. Chem. Eng.*, vol. 7, no. 3, p. 103080, 2019, doi: 10.1016/j.jece.2019.103080.

[27] Wolters, J., Tagliavini, M., and Schäfer, A. I., "Removal of steroid hormone micropollutants by UF-PBSAC composite in presence of organic matter," *J. Membr. Sci.*, vol. 592, p. 117315, 2019, doi: 10.1016/j.memsci.2019.117315.

[28] Zhang, J., Nguyen, M. N., Li, Y., Yang, C., and Schäfer, A. I., "Steroid hormone micropollutant removal from water with activated carbon fiber-ultrafiltration composite membranes," *J. Hazard. Mater.*, vol. 391, p. 122020, 2020, doi: 10.1016/j.jhazmat.2020.122020.

[29] Kaminska, G., Bohdziewicz, J., Calvo, J. I., Prádanos, P., Palacio, L., and Hernández, A., "Fabrication and characterization of polyethersulfone nanocomposite membranes for the removal of endocrine disrupting micropollutants from wastewater. Mechanisms and performance," *J. Membr. Sci.*, vol. 493, pp. 66–79, 2015, doi: 10.1016/j.memsci.2015.05.047.

[30] Liao, Z. *et al.,* "Low pressure operated ultrafiltration membrane with integration of hollow mesoporous carbon nanospheres for effective removal of micropollutants," *J. Hazard. Mater.*, vol. 397, p. 122779, 2020, doi: 10.1016/j.jhazmat.2020.122779.

[31] Tagliavini, M. and Schäfer, A. I., "Removal of steroid micropollutants by polymer-based spherical activated carbon (PBSAC) assisted membrane filtration," *J. Hazard. Mater.*, vol. 353, pp. 514–521, 2018, doi: 10.1016/j.jhazmat.2018.03.032.

[32] Back, J., Brandstätter, R., Spruck, M., Koch, M., Penner, S., and Rupprich, M., "Parameter Screening of PVDF/PVP Multi-Channel Capillary Membranes," *Polymers*, vol. 11, no. 3, p. 463, 2019, doi: 10.3390/polym11030463.

[33] Quilitzsch, M., Osmond, R., Krug, M., Heijnen, M., and Ulbricht, M., "Macro-initiator mediated surface selective functionalization of ultrafiltration membranes with anti-fouling hydrogel layers applicable to ready-to-use capillary membrane modules," *J. Membr. Sci.*, vol. 518, pp. 328–337, 2016, doi: 10.1016/j.memsci.2016.07.007.

[34] Back, J., Spruck, M., Koch, M., Mayr, L., Penner, S., and Rupprich, M., "Poly(piperazine-amide)/PES Composite Multi-Channel Capillary Membranes for Low-Pressure Nanofiltration," *Polymers*, vol. 9, no. 12, p. 654, 2017, doi: 10.3390/polym9120654.

[35] Back, J. O., Hupfauf, B., Rößler, A., Penner, S., and Rupprich, M., "Adsorptive removal of micropollutants from wastewater with floating-fixed-bed gasification char," *J. Environ. Chem. Eng.*, vol. 8, no. 3, p. 103757, 2020, doi: 10.1016/j.jece.2020.103757.

[36] Ousman, M. and Bennasar, M., "Determination of various hydraulic resistances during cross-flow filtration of a starch grain suspension through inorganic membranes," *J. Membr. Sci.*, vol. 105, 1-2, pp. 1–21, 1995, doi: 10.1016/0376-7388(94)00266-2.

[37] Ho and Zydney, "A Combined Pore Blockage and Cake Filtration Model for Protein Fouling during Microfiltration," *J. Colloid Interface Sci.*, vol. 232, no. 2, pp. 389–399, 2000, doi: 10.1006/jcis.2000.7231.

[38] Furukawa, T., Kokubo, K., Nakamura, K., and Matsumoto, K., "Modeling of the permeate flux decline during MF and UF cross-flow filtration of soy sauce lees," *J. Membr. Sci.*, vol. 322, no. 2, pp. 491–502, 2008, doi: 10.1016/j.memsci.2008.05.068.

[39] Vela, M. C. V., Blanco, S. Á., García, J. L., and Rodríguez, E. B., "Analysis of membrane pore blocking models applied to the ultrafiltration of PEG," *Sep. Purif. Technol.*, vol. 62, no. 3, pp. 489–498, 2008, doi: 10.1016/j.seppur.2008.02.028.

[40] Sun, Y. *et al.,* "Membrane fouling mechanisms and permeate flux decline model in soy sauce microfiltration," *J. Food Process Eng.*, vol. 41, no. 1, e12599, 2018, doi: 10.1111/jfpe.12599.

[41] R core team, *R: A language and environment for statistical computing*, 2020. Accessed: Aug. 5 2020. [Online]. Available: https://www.r-project.org/

[42] Torras, C., Ferrando, F., Paltakari, J., and Garciavalls, R., "Performance, morphology and tensile characterization of activated carbon composite membranes for the synthesis of enzyme membrane reactors," *J. Membr. Sci.*, vol. 282, 1-2, pp. 149–161, 2006, doi: 10.1016/j.memsci.2006.05.018.

[43] Margot, J., Rossi, L., Barry, D. A., and Holliger, C., "A review of the fate of micropollutants in wastewater treatment plants," *WIREs Water*, vol. 2, no. 5, pp. 457–487, 2015, doi: 10.1002/wat2.1090.